Journal of Molecular Neuroscience (2022) 72:401–409
https://doi.org/10.1007/s12031-021-01960-1

Investigation of the Role of Induced Overexpression of the Isolated Secreted Klotho on the A-172 Human Glioblastoma Cells

Vsevolod V. Melekhin[1,2,3] · Alexander I. Ponomarev[1,2,4] · Maria A. Desyatova[1] · Oleg G. Makeev[1,2]

Received: 15 June 2021 / Accepted: 19 December 2021 / Published online: 3 February 2022

Abstract

Klotho gene, identified in 1997 as an anti-aging gene, can manufacture two protein products: transmembrane and secreted forms. The later research revealed the involvement of klotho in carcinogenesis. However, little is known about the action of different Klotho forms on antitumor effects is still. The purpose of this article is to evaluate the effect of isolated secreted Klotho overexpression on the growth features of human glioblastoma cell line A-172.

A-172 was transfected by a plasmid vector incorporating secreted Klotho sequence by the liposomal method. Overexpression assay was carried out quantitatively on both mRNA and protein using RT-qPCR and ELISA, correspondingly. It was shown that the relative expression of secreted Klotho in the experimental group was significantly higher than in the untransfected group by both methods ($p < 0.001$). At the same time, the growth curves and MTT proliferation assay demonstrated significantly decreased values under induced overexpression ($p < 0.01$). The increased amount of cells with activated caspases and annexin V ($p < 0.001$) corresponded with the expression of secreted Klotho. This mechanism, as suggested, maybe causative of the observed effects.

Keywords Secreted Klotho · Lipofection · Plasmid vector · Gene expression · Apoptosis

Introduction

Klotho gene was discovered in 1997 as an anti-aging gene (Kuro-o et al. 1997). The Klotho gene has two mRNA first variant encodes a longer transmembrane form (mKL) of the protein, while the second splicing option results in a truncated secreted one (sKL). The mKL is a single-pass transmembrane protein that includes 1012 amino acids (around 135 kDa). The mKL comprises a large extracellular domain with two homologous KL1 and KL2, a transmembrane domain and a short intracellular domain, while the sKL is twice shorter and includes 549 amino acids (around 65 kDa). Although there is an almost twofold difference in amino acid length, mRNAs of these proteins are poorly distinguishable, and the insertion of 45 bp is the mere of the established. The latter is due to alternative splicing and results in the nonsense (stop) codon; thus, the translated protein comprises three exons (Matsumura et al. 1998). It should be noted that mKL might also be shed, resulting in the shKL protein. The latter is capable of getting into the bloodstream, cerebrospinal fluid, and urine (Chen et al. 2014).

The involvement of Klotho in carcinogenesis has been shown in breast cancer (Rubinek et al. 2012; Wolf et al. 2010, 2008), lung cancer (Chen et al. 2012, 2010; Wang et al. 2013), liver cancer (Chen et al. 2013; Tang et al. 2016; Xie et al. 2013; Sun et al. 2015), and other oncological diseases. For example, Klotho expression in the tumor was examined and compared with similar healthy surrounding tissue (Rubinek et al. 2012; Chen et al. 2013; Tang et al. 2016; Yan et al. 2017). Also, the assessment of the methylation status of the promoter region is carried out (Rubinek

Vsevolod V. Melekhin and Alexander I. Ponomarev contributed equally to this work

✉ Alexander I. Ponomarev
ponomareff@yandex.ru

1 Department of Biology, Ural State Medical University, Ekaterinburg, Russia

2 Department of Gene and Cell Therapy, Institute for Medical Cell Technologies, Ekaterinburg, Russia

3 Labratory of the Primary Bio Screening, Cell and Gene Technologies, Chemical Technology Institute, Ural Federal University, Ekaterinburg, Russia

4 Molecular Biology, Immunophenotyping, and Pathomorphology Department, Regional Children's Hospital, Ekaterinburg, Russia

et al. 2012; Xie et al. 2013; Lee et al. 2010). Moreover, its involvement in carcinogenesis was the scope of many studies with both gene knockout and overexpression. The means of genetic transfection or adding purified Klotho protein to the cell cultures are employed to achieve these tasks and are usually followed by evaluating the cell growth features (Chen et al. 2012, 2010; Tang et al. 2016; Yan et al. 2017; Lee et al. 2010).

In general, the data collected up to date justify the decrease of Klotho expression in tumor cells compared to the surrounding normal tissue. The latter corresponds with initial observation in breast cancer. It is also assumed that the methylation of the gene promoter and involvement of insulin and insulin-like growth factor 1 (IGF-1) play a partial role in the antitumor effect of the Klotho gene (Wolf et al. 2008). The following studies suggest the effect of insulin/IGF-1 on the canonical proteins of the Wnt family (Tang et al. 2016; Sun et al. 2015) and PI3K/AKT pathway (Li et al. 2014) and its possible contribution to more aggressive neoplasia. The involvement of Klotho in apoptotic proteins of the Bcl-2 and Bax family and many others was also determined (Chen et al. 2010). It is worth noting that the research endeavors used to reveal Klotho features have not attempted to research an isolated action of various forms of the protein and to compare them, rather predominantly focused on mKL(Wolf et al. 2008). Nevertheless, some previously conducted research showed data regarding features of recombinant Klotho lacking KL1 domain (516 amino acids) added to cancer cell lines (Chen et al. 2012; Tang et al. 2016; Lee et al. 2010).

Even though much data is available associating Klotho with carcinogenesis, there are no studies aimed to investigate the differently encoded Klotho proteins in neoplasia, yet it is known the mKL forms a complex with the FGF receptor and acts as a co-receptor for FGF23, thus affecting phosphate metabolism, whereas the functional characteristics of sKL remain unclear (Hu et al. 2013). Of the general assumptions that the sKL is released into the microenvironment and circulates as a humoral factor, causing auto- and paracrine effects on cells (Matsumura et al. 1998; Chen et al. 2014). Thus, the sKL may have broad targeting, affecting more than one cell.

Recent studies have demonstrated that Klotho is involved in carcinogenesis in glioblastoma cells. However, it revealed ambiguous causative patchwork between Klotho expression, methylation of the promoter region, and patients' survival rate add value as itself and need to be deciphered (Peshes-Yeloz et al. 2019). It contributes to additional research aimed at clarifying different aspects of the Klotho on glioblastoma cells. There is evidence that Klotho can inhibit the viability of A-172 cells. In particular, some studies have shown that A-172 cells are sensitive to changes in the PI3K / AKT signaling pathway (Kalhori et al. 2019), Wnt expression (Kirikoshi et al. 2001), and Bax and Bcl-2 proteins (Chen et al. 2007; Dabili et al. 2019) affected by Klotho. Thus, A-172 might represent a significant interest in the consecutive study of the various Klotho forms.

The present study aims to examine the effect of an isolated overexpression of the sKL on the growth features and apoptosis of the A-172 human glioblastoma cell line and provides a glimpse of a mechanism to investigate further profoundly.

Materials and Methods

Cell Culture and Transfection

Studies were carried out on the cell cultures of human glioblastoma line A-172 (ATCC CRL 1620) (Giard et al. 1973) obtained from the Institute of Cytology RAS (St. Petersburg, Russia). Cells were cultured under 95% humidity, 5% CO_2, and 37 °C on Dulbecco's Modified Eagle's Medium/Ham F-12 (Sigma Aldrich, USA) mixed medium containing 10% bovine fetal serum.

Cultures were pre-sown in 25 cm2 vials (Orange Scientific, Belgium) or flat-bottomed 96-well plates (Orange Scientific, Belgium). Each group consisted of 7–10 replicates for both growth curves and apoptosis or 30 replicates for the MTT. Transfection was carried out with Lipofectamine 2000 polycationic lipid complex (Invitrogen, USA). Cell cultures reaching 60% of the confluence index were employed for further processing. The transfection mixture included 0.2 µg pDNA/sKL or pcDNA3.1/V5/His-TOPO for experiment and control series correspondingly. Lipofectamine 2000 in a volume of 0.5 µl per well of a 96-well plate and 8 µg DNA and 20 µl per 25 cm2 culture flask was used. The cells were incubated in the transfection mixture for 18 h, and then, the medium in cultures was changed into a standard growth medium (DMEM/Ham F-12 with 10% FBS).

pDNA Extraction, Qualitative and Quantitative Assays, Control Vector Development

The Klotho plasmid (secreted form) was kindly provided by the Hal Dietz laboratory of Johns Hopkins University (Addgene plasmid # 17,713) (Arking et al. 2002). It should be mentioned that the applied genetic construct included only three Klotho exons and was incapable of producing the full-length protein. The circular pcDNA3.1/V5/His-TOPO plasmid with the β-galactosidase blank sequence was made by inserting the corresponding gene into a linearized plasmid and used to transfect the control group (ThermoFisher, USA). E.coli were transformed with the blank genetic vector using the same heat shock approach as was used for the experimental group and subcloned under the standard

conditions in LB media. Plasmid DNA (pDNA) was then isolated from the E. coli using the Miniprep Kit (Zymo Research, USA) according to the manufacturer's protocol. The blank plasmid was then amplified and sequenced using the approach described below. The alignment of the blank incorporated lacZ gene to the reference sequence was performed using BLAST (Table S1, Suppl.).

Quantitative calculation of pDNA was performed on a spectrophotometer (BIO-RAD, USA) at a wavelength of 260 nm. Qualitative analysis was carried out according to the ratio of A260/A280. Samples were considered appropriate at A260/A280 = 1.8 ± 0.1. A series of dilutions were prepared for subsequent PCR in qualitative and quantitative formats with a known copy of 1 µl of solution: 1×10^4, 1×10^5, and 1×10^6. The plasmid DNA copy number of each dilution was also established using droplet digital PCR (BIO-RAD, USA) to quantify the exact number precisely. The least one was applied to qualitative PCR with custom-made primers spanning the junction of the first two exons of the Klotho (Table 1). The expected size of the product synthesized from these primers is 103 bp. Reactions were carried out in twofold buffer (Fermentas, USA), 25 µM of each primer, and 2.5 U Dream Taq polymerase (Fermentas, USA). The following thermal cycling parameters were used: 95 °C for 2 min and then 35 cycles: 95 °C for 15 s, 62 °C for 15 s, and final elongation at 72 °C for 7 min. The specificity of the reaction was evaluated by PAG electrophoresis. The main criterion was the absence of fragments of length other than 103 bp. Fragments of the desired size were cut out, and DNA was extracted and purified from the gel. Sanger sequencing was performed for three samples of both control and experimental vectors in forward and reverse directions.

Total RNA Isolation and Reverse Transcription, Gene Expression Assay

The transfected cultures were washed three times with PBS solution and removed from the culture flasks according to a standard procedure using a 0.25% Trypsin solution. The resulting suspensions were centrifuged at 200 g for 5 min, and the pellet was re-suspended in 200 µl of PBS solution and then mixed with TRI Reagent solution (MRC, USA) in a ratio of 1: 4, and then, the total RNA was isolated according to the manufacturer's instructions. Dry-precipitated RNA was dissolved in 10 µl of Rnase free water (Qiagen, Netherlands); the concentration was measured. A reverse transcription reaction was performed in 1 µg of total RNA at 37 °C for 60 min using random hexamers in 10 µl of a master mix (Promega, USA), consisting of 5X reverse transcription buffer, 10 mM dNTP, 100 µM random primer, 5 U MMLV reverse transcriptase, 1 U RNase inhibitor. For the subsequent qPCR reactions, 2.5 µl of cDNA was used per reaction.

Gene expression was studied by the RT-qPCR (reverse transcriptase quantitative PCR). The calibration curves were plotted using serial dilutions, prepared during the isolation step of pDNA/sKL with precisely characterized copy numbers. The sKL was detected by primers used for qualitative PCR, hydrolysis probe labeled with FAM (green channel) was added (Table 1). Reactions were performed in a uniplex format using a master mix (Promega) consisting of 5X buffer, 10 mM dNTP, 50 mM Mg^{2+}, 6.5 µM of each primer, 5 µM probe, ddH_20, and 2.5 U GoTaq polymerase and pDNA of the desired copy number. Amplification and fluorescence detection were performed on a LightCycler 96 instrument (Roche, Switzerland) with thermal cycling parameters: 95 °C for 2 min and then 45 cycles: 95 °C for 15 s, 62 °C for 15 s. The analysis of the curves raw data, the recording of Cq, and the plotting of calibration curves were performed in the LightCycler 96 SW 1.1 software.

Abelson gene (*ABL1*) was used as a reference gene due to its relatively stable expression in different cells and lack of dependency on various treatment factors. Abl1 detection was performed using the primers and FAM labeled hydrolysis probe (Table 1). Calibration curves for the *ABL1* gene were plotted using commercial *ABL1* Control gene plasmids with a characterized copy number of 1×10^4, 1×10^5, and 1×10^6(Qiagen, Netherlands). The efficiency of amplification of the sKL and Abl1 fragments was estimated by the formula: $10 - 1$ / slope $- 1$. Gene expression assay in both experimental and control cultures was performed according to the described procedure. The absolute number of the sKL and Abl1 genes was found in copies per reaction volume. The results of sKL expression were expressed as relative to *ABL1*.

Table 1 Sequences of oligonucleotides

Gene	Type	Sequence (5′-3′)
ABL1	Forw. primer	AGCTCCGGGTCTTAGGCTAT
	Rev. primer	TAGTTGTTGGGACCCAGCC
	Probe	CCATTTTTGGTTTGGTTTACACCATT
Klotho	Forw. primer	CACAACCTCCTCCTGGCTCAT
	Rev. primer	TCCAGTGAGAGCTTAGGGCA
	Probe	CCGTCCCACTCAGGGAGGTCA

Protein Expression Assay

The concentration of Klotho protein in cell cultures was also measured to assess sKL overexpression directly. As the cells secreted the sKL into the microenvironment, we carried out an expression assay in both cell lysates and culture medium. The concentration of the sKL protein was determined using a kit for ELISA on the human Klotho protein (Cloud-Clone Corp., USA). The analysis was carried out by

the manufacturer's protocol. The optical density obtained at a wavelength of 450 nm was used to determine the protein concentration from the calibration data of standard dilutions represented by the regression equation.

MTT Test

MTT test was performed to evaluate the impact of sKL on the viability and proliferation; the test cells were cultured in 96-well plates at a seed concentration of 8×10^3 cells per well, followed by transfection. The viability evaluation was carried out after washing off the transfection mixture in 24, 48, and 72 h. The addition of MTT [3-(4,5-dimethylthiazol-2,5-diphenyltetrazolium bromide, 20 µl, 10 mg/ml; Sigma Aldrich, USA] was followed by incubation of cell cultures for 4 h. Then, the supernatant was removed from each well, and 200 µl of Me_2SO/2-propanol solution (1:1 ratio) was added into each well for 10 min. The calorimetric assay was carried out on a Multiscan Go tablet spectrophotometer (Thermo Fisher Scientific, Finland). The optical density was measured at 570 nm.

Growth Curves

Cultures were transferred into culture flasks with an area of 25 cm^2 (Orange Scientific, Belgium) with a seed concentration equal to 4×10^3 cells/cm^2. Cells were subjected to transfection (experimental group) or the transfection mixture with pcDNA3.1/V5/His-TOPO blank plasmid (control group). The cultures were consecutively removed from the experiment after transfection in 24, 48, and 72 h with the number of cells counted by the Scepter automatic cell counter (Millipore, USA).

Apoptosis

A-172 cells were cultured in 25 cm^2 culture flasks followed by transfection. In 48 h, after transfection, the cells were stained with fluorescent dye using the FAM-FLICA (Fluorescent-Labeled Inhibitor of Caspases) Poly Caspase Assay Kit (Novus, USA) according to the manufacturer's recommendations. Moreover, the apoptosis machinery was also assessed using fluorescent staining with the Annexin V Fitc Staining kit (Sigma Aldrich, USA).

The use of additional staining with propidium iodide solution enabled the differentiation of necrotic cells from apoptotic ones. The relative number of caspase-active cells and annexin V positive cells was determined by counting with a ZOE fluorescent cell imager (BIO-RAD, USA) via various fluorescent filters on the Fuchs-Rosenthal counting chamber.

Statistics

The data is presented as an arithmetic means of ± SD. Statistical analysis was carried out in the R version 4.0.2 (R Foundation for Statistical Computing, Austria, Vienna). Shapiro–Wilk's test determined the distribution of numeric values. Bartlett's test assessed the difference of the pairwise variance. The Student's *t* test was used to determine the statistically significant differences between the two groups. The $p < 0.05$ was taken as statistically significant. The Y-intercept and slope coefficients for calculating gene copy numbers were obtained by the linear regression method. The copy numbers were calculated with the coefficients of determination (R^2) ≥ 0.98.

Results

The designed oligos set's specificity and optimal annealing temperature were evaluated after a one-round PCR, followed by visualizing heterogeneous reaction products in PAGE. It was shown that this custom-made set of both primers and probes achieved a lack of non-specific products with both plasmid and genomic DNA. Increased accumulation of the PCR product was observed at an annealing temperature of 62 °C in comparison with 58 °C and 64 °C. The resulting size of PCR products was similar to the expected of 103 bp (Fig. S1A, Suppl.)

The concordance of the obtained and expected products was established by direct sequencing. Two short sequences of 68 (sense) and 64 (anti-sense) bp were obtained from forward and reverse primers, respectively. The complete identity of the Klotho mRNA was established by comparing it with the reference sequences in both single and consensus variants. The consensus sequence was expectedly located at the junction of the first and second exons of the gene. It enabled detecting pDNA and mRNA of the sKL, plot calibration curves, and gene expression assay (Fig. S1B, Table S1, Suppl.).

The qPCR on plasmid DNA samples with a characterized copy number allowed us to plot standard calibration curves and create regression curves ($R^2 = 0.99$) to calculate the absolute number of copies: $Lg_{\text{number of copies}} = (\text{Ct-Y-intercept})/\text{slope}$, where Ct is the value of the threshold reaction cycle (Fig. S1C, Suppl.).

The sKL and *ABL1* fragments amplification efficiencies were commensurable and equal to 91 and 99%, respectively. Therefore, according to the MIQE criteria (Bustin et al. 2009), information regarding the qPCR technique and quantification data suggests that technology for the expression assay was proven as appropriate, so according to RT-qPCR data shown in Fig. 1A, the relative expression in the

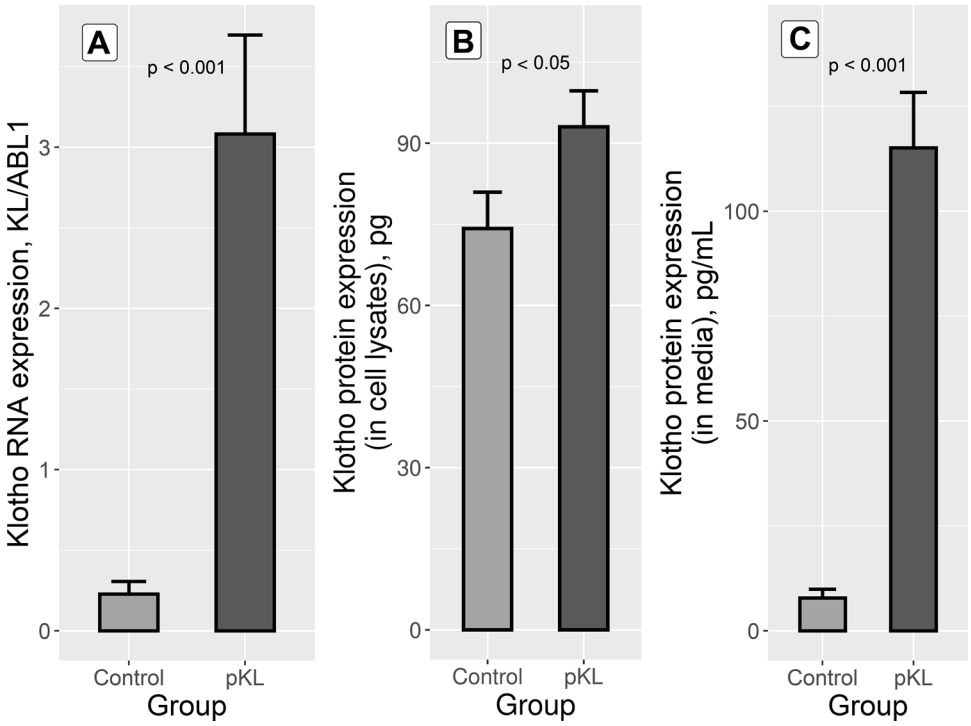

Fig. 1 Induction of overexpression of the Klotho gene. **A** Relative Klotho gene expression in A-172 human glioblastoma culture cells, *KL/ABL1* ($n=3$, mean ± SD). **B** Concentrations of Klotho protein in cell lysates (Klotho, pg/total protein, μg; $n=3$, mean ± SD). **C** Concentrations of Klotho protein in medium (Klotho, pg; $n=3$, mean ± SD)

control group was on average 13.55 times less than in the experimental group ($p<0.001$).

Analysis of Klotho protein overexpression revealed concentration in cell lysates 74.22 ± 6.73 in the control group and 93.03 ± 6.65 in the experimental group (pg of Klotho protein/μg of total protein). The revealed differences also had a significance, $p=0.026$ (Fig. 1B). Likewise, higher significant differences were detected in the culture medium, likely due to the release of the protein outwards (Fig. 1C). Thus, the concentration of the sKL in control was 7.82 ± 2.11 pg/mL compared to experimental: 115.1 ± 13.24 pg/mL. Therefore, the cell transfection per se facilitated an increased amount of sKL over 14 times ($p<0.001$). The latter has almost the same magnitude as RT-qPCR overexpression (14.72 vs. 13.55) data pointing out that the total mRNA was translated into protein.

To examine if sKL overexpression affects glioblastoma cells' growth characteristics, we carried out three tests: MTT, growth curves, and apoptosis.

MTT

The results of the MTT test (Fig. 2A) did not reveal significant differences in the experimental and control groups after transfection in 24 h. The average OD570 in the experimental group was lower by more than 4% than in the control group (0.8 ± 0.09 vs. 0.83 ± 0.09, $p=0.15$). However, the experimental group was already 4.35% lower than the control at the following point, indicating that significance was achieved (1.2 ± 0.1 vs. 1.26 ± 0.1, $p=0.04$). Finally, the 72 h revealed an extra difference, so OD570 in the experimental group turned out to be 8% lower than in the control group (1.95 ± 0.27 vs. 2.12 ± 0.21, $p<0.01$).

Growth Curves

In general, growth curve plots (Fig. 2B) were well correlated with the MTT data. At 24 h, no significant differences were registered. The number of cells in the experimental group was lower only by 5.24% than in control (19.63 ± 1.39 vs. 20.71 ± 1.97, $p=0.26$). However, 48 h after transfection in the experimental group, the number of cells decreased by 10.87% compared to control (27.89 ± 4.6 vs. 31.29 ± 2.21, $p=0.075$). Finally, at 72 h, the number of cells in the experimental group was already 19.29% lower than in control (37.77 ± 6.39 vs. 46.8 ± 3.92, $p<0.01$).

Apoptosis

The number of cells with activated caspases under the sKL overexpression significantly increased (Fig. 3A). In the experimental group, the number of caspase-active cells was equal to 6.71%. In the control group, this number was about 4.1% (6.71 ± 1.15 vs. 4.1 ± 0.91, $p<0.001$). Thus, although the absolute count was moderate, higher apoptosis under sKL overexpression could be observed, with a 1.63-fold increase.

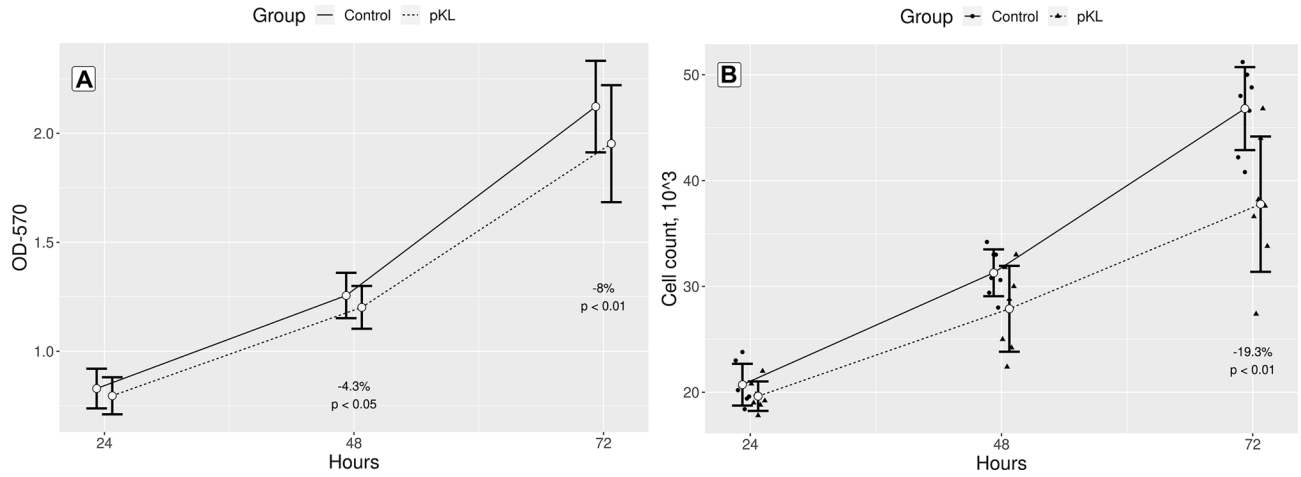

Fig. 2 Effects of sKL overexpression on proliferation and viability of human glioblastoma cells. **A** MTT test ($n=30$, mean ± SD). **B** Growth curves, cell count × 10^3/sm^2 ($n=7$, mean ± SD)

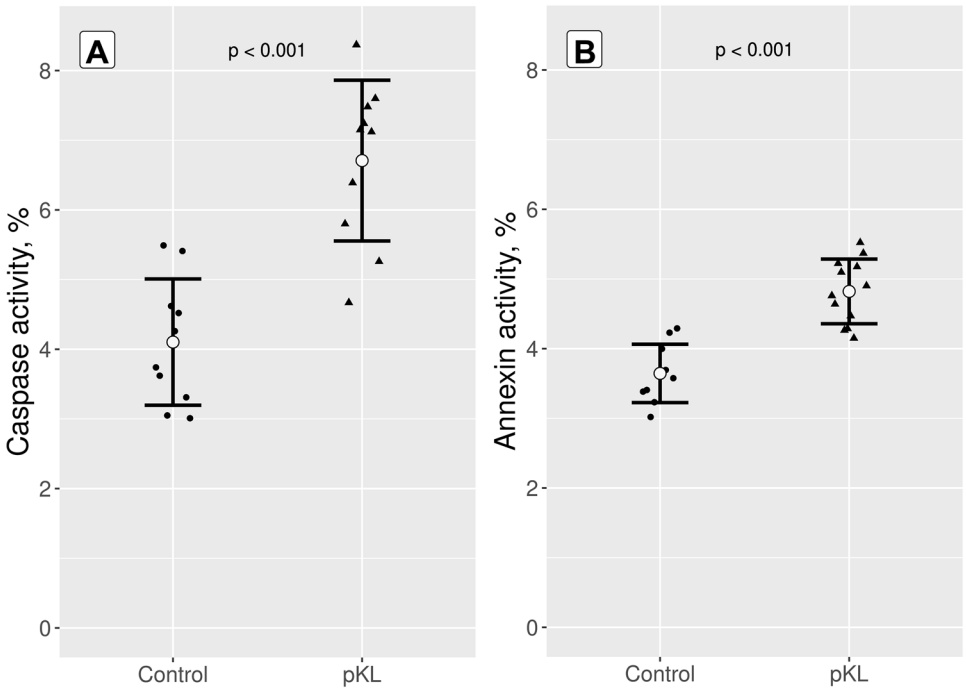

Fig. 3 Effects of sKL overexpression on apoptosis. **A** The ratio of cells with increased caspase activity in the experimental and control groups ($n=10$, mean ± SD). **B** The relative amount of Annexin-V-positive cells in the experimental and control groups ($n=10$ control, $n=12$ experimental, mean ± SD)

In addition, a significant number of apoptotic cells were recorded using Annexin V staining. As shown in the diagram (Fig. 3B), the control group's average percentage of apoptotic cells was 3.64 ± 0.42% compared to 4.82 ± 0.46% in the experimental group (1.32-fold higher, $p<0.001$). Thus, as in the RT-qPCR vs. protein expression comparison mentioned above, the given numbers (1.32 vs. 1.63) correspond and show similar magnitude.

Discussion

In the present study, the liposomal transfection of a plasmid containing a secreted form of Klotho protein induced a 13.55 times higher expression compared to the control as detected by RT-qPCR. However, it is of particular importance to confirm this value by direct protein measurement. Therefore, we performed an ELISA as a verification tool.

Eventually, revealed sKL mRNA overexpression is confirmed by direct protein measurements demonstrating an increase of sKL protein in the experimental group by more than 25% in cell lysates and by 14.72 times in culture medium. Meanwhile, the main idea of the research was to discover whether the isolated overexpression of the separate sKL was capable of inhibiting the growth of A-172 and of providing some glimpse of a possible mechanism to investigate further. To address this problem, we inspected the growth curves, MTT plots, and apoptosis (Fig. 2). On the one hand, we showed the consistency between tests conducted. By contrast, some absolute counts (caspase-cells) demonstrated slight differences, likely indicating that more complicated machinery is recruited in cells' growth inhibition than apoptosis as sole. Nevertheless, we suggest providing a quick overview of the possible apoptotic mechanisms involved in antitumor action (based on the previous studies) and its consistency with our findings.

Four independently carried out tests demonstrated a statistically significant effect with a high degree of reliability (in all cases, the p value was < 0.01). At the same moment, the most pronounced effect was registered at caspases activity assessment and annexin V (in both cases, $p < 0.001$). However, in general, the increase of the cell numbers, supposedly in apoptosis, turned out to be moderate (4% vs. 6.7%). It is noteworthy that we obtained comparable data upon analyzing annexin V. It might be due to some intracellular mechanism capable of partially blocking the sKL-induced apoptosis in glioblastoma cells. However, the given hypothesis could be considered assumptive and require a more detailed study. Likewise, it is known that an increase in the activity of caspases does not always indicate the initiation of programmed cell death. For example, activated caspases may not contribute to cell death if the action of these proteases is blocked by apoptosis inhibitor proteins (PAIs) (Shi 2004; Vaux and Silke 2005). The published research data indicate the involvement of some proteins in the initiation of the mitochondrial pathway of apoptosis in klotho-mediated mechanisms for the suppression of cell viability. For instance, it was shown the participation of proteins of the Bcl-2 and Bax family in klotho-mediated antitumor activity using lung cancer as an example (Chen et al. 2010). The activity of well-studied initiator and effector caspases and caspases − 1, − 4, and − 5 possibly associated with inflammatory processes or unknown functions of these compounds are discussed. Therefore, the induction of apoptosis in cells is only one of the possible options for suppressing the viability of a human glioblastoma cell culture.

The next issue is differences in significance upon analyzing similar plot points shown in Fig. 2. As it can be seen, the MTT test showed significant differences already at the second and third-time marks (48, 72 h) of the experiment, while the growth curves showed significance only on the third day (72 h). We assume that this may be explained by various ways to statistical data analysis in these experiments. The growth curves were plotted based on data of 7–10 cultures in each group, while the sample during the MTT test had 60 independent observations in both groups. Although the same parametric approaches were performed upon statistical calculations, it should be noted that the applied statistical power of any test relies, among the others, on the sample size. Therefore, we argue that the MTT test provides more reliable values of the effect of sKL on the proliferation of A-172.

Meanwhile, overexpression of Klotho can induce the development of other regulatory disorders in the cells. According to several studies, the effect of Klotho on the signal interactions of insulin and insulin-like growth factor 1 was determined to possibly influence cell antioxidant protection (Li et al. 2014; Shu et al. 2013; Lu et al. 2008). It is also assumed that there is a correlation between various miRNAs that may be involved in the development of carcinogenesis. In particular, some studies have shown the correlation between the expression of the Klotho gene and miR-339 and miR-556 (Mehi et al. 2014), miR-199a-5p (He et al. 2014), and miR-10b (Pan et al. 2015).

It should be mentioned that the current research has demonstrated for the first time the effect of the gene overexpression of the secreted (3-exon) Klotho protein on the growth of human glioblastoma cells. In the previously reported studies, the effect of the full, i.e., a 5-exon form of the protein, was investigated (Wang et al. 2013; Chen et al. 2013; Shu et al. 2013). Meanwhile, to assess Klotho gene expression by the RT-qPCR method, we recruited ddPCR for precise calibration of sKL copies and designed our own primers and probe, which considerably increases the specificity of the assay. The addition of mentioned above, as well as detection of expression of a reference gene, makes an assay more accurate and sensitive as well as enabled to observe almost complete concordance between qPCR and ELISA (13.55 and 14.72 times). It is noteworthy that the existing approaches applied to detect the mKL use primers targeting gene regions of 4 and 5 exons and cannot be used for the secreted form since these regions are absent in the given (sKL) genetic construct. For example, the quantification approach described above, as well as full-length plasmid, was used by Chen et al. (Chen et al. 2010).

In general, the current research results correlate with the results described in the articles on the subject. The methods of growth curves plotting and the MTT test demonstrated inhibition of cell proliferation combined with significant activation of caspases. More detailed research is required to form the hypothesis of Klotho involvement in the mechanisms of carcinogenesis in glioblastoma cells.

Supplementary Information The online version contains supplementary material available at https://doi.org/10.1007/s12031-021-01960-1.

Acknowledgements Authors also express our gratitude to Gleb Derbyshev, Anna Shcheglova, Elisaveta Yakovleva for all kinds of technical assistance accompanying most of the experimental procedures related to this article.

Author Contribution All authors contributed to the study's conception and design. Material preparation, data collection, and analysis were performed by VM, AP, and MD. The first draft of the manuscript was written by VM, AP, and OG, and all authors commented on previous versions of the manuscript. All authors read and approved the final manuscript.

Funding This study was in part supported by the grant of The Russian Ministry of Health (AAAA-A18-118041890078–5) as a part of the project "Investigation of the role of the Klotho genes family in carcinogenesis." The funding body had no role in the design of the study and collection, analysis, and interpretation of data, and in writing the manuscript.

Data Availability All data related to this article, as well as additional figures and tables, are available in supplementary material provided with this article.

Declarations

Ethics Approval and Consent to Participate Not applicable.

Consent for Publication Not applicable.

Competing Interests The authors declare no competing interests.

References

Arking DE, Krebsova A, Macek M, Arking A, Mian IS, Fried L et al (2002) Association of human aging with a functional variant of klotho. Proc Natl Acad Sci 99(2):856–861. https://doi.org/10.1073/pnas.022484299

Bustin SA, Benes V, Garson JA, Hellemans J, Huggett J, Kubista M et al (2009) The MIQE guidelines: minimum information for publication of quantitative real-time PCR experiments. Clinical Chem 55(4):611–622. https://doi.org/10.1373/clinchem.2008.112797 Published March 2009

Chen B, Ma X, Liu S, Zhao W, Wu J (2012) Inhibition of lung cancer cells growth, motility and induction of apoptosis by Klotho, a novel secreted Wnt antagonist, in a dose-dependent manner. Cancer Biol Ther 13(12):1221–1228. https://doi.org/10.4161/cbt.21420

Chen B, Wang X, Zhao W, Wu J (2010) Klotho inhibits growth and promotes apoptosis in human lung cancer cell line A549. J Exp Clin Cancer Res 29(1):99. https://doi.org/10.1186/1756-9966-29-99

Chen CD, Tung TY, Liang J, Zeldich E, Zhou TBT, Turk BE et al (2014) Identification of cleavage sites leading to the shed form of the anti-aging protein klotho. Biochemistry 53(34):5579–5587. https://doi.org/10.1021/bi500409n

Chen JC, Chen Y, Su YH, Tseng SH (2007) Celecoxib increased expression of 14-3-3U and induced apoptosis of glioma cells. Anticancer Res 27(4B):2547–2554

Chen L, Liu H, Liu J, Zhu Y, Xu L, He H et al (2013) Klotho endows hepatoma cells with resistance to anoikis via VEGFR2/PAK1 activation in hepatocellular carcinoma. PLoS One 8(3):e58413. https://doi.org/10.1371/journal.pone.0058413

Dabili S, Fallah S, Aein M, Vatannejad A, Panahi G, Fadaei R et al (2019) Survey of the effect of doxorubicin and flavonoid extract of white Morus alba leaf on apoptosis induction in a-172 GBM cell line. Arch Physiol Biochem 125(2):136–141. https://doi.org/10.1080/13813455.2018.1441871

Giard DJ, Aaronson SA, Todaro GJ, Arnstein P, Kersey JH, Dosik H et al (1973) In vitro cultivation of human tumors: establishment of cell lines derived from a series of solid tumors. J Natl Cancer Inst 51(5):1417–1423

He XJ, Ma YY, Yu S, Jiang XT, Lu YD, Tao L (2014) Up-regulated miR-199a-5p in gastric cancer functions as an oncogene and targets klotho. BMC Cancer 14(1):218. https://doi.org/10.1186/1471-2407-14-218

Hu MC, Shiizaki K, Kuro OM, Moe OW (2013) Fibroblast growth factor 23 and Klotho: physiology and pathophysiology of an endocrine network of mineral metabolism. Annual Rev Physiol 75:503–533. https://doi.org/10.1146/annurev-physiol-030212-183727

Kalhori MR, Irani S, Soleimani M, Arefian E, Kouhkan F (2019) The effect of miR-579 on the PI3K/AKT pathway in human glioblastoma PTEN mutant cell lines. J Cell Biochem 120(10):16760–16774. https://doi.org/10.1002/jcb.28935

Kirikoshi H, Inoue S, Sekihara H, Katoh M (2001) Expression of WNT10A in human cancer. Int J Oncol 19(5):997–1001. https://doi.org/10.3892/ijo.19.5.997

Kuro-o M, Matsumura Y, Aizawa H, Kawaguchi H, Suga T, Utsugi T et al (1997) Mutation of the mouse klotho gene leads to a syndrome resembling aging. Nature 390(6655):45–51. https://doi.org/10.1038/36285

Lee J, Jeong DJ, Kim J, Lee S, Park JH, Chang B et al (2010) The anti-aging gene KLOTHO is a novel target for epigenetic silencing in human cervical carcinoma. Mol Cancer 9(1):109. https://doi.org/10.1186/1476-4598-9-109

Li XX, Huang LY, Peng JJ, Liang L, Shi DB, Zheng HT et al (2014) Klotho suppresses growth and invasion of colon cancer cells through inhibition of IGF1R-mediated PI3K/AKT pathway. Int J Oncol 45(2):611–618. https://doi.org/10.3892/ijo.2014.2430

Lu L, Katsaros D, Wiley A, Rigault de la Longrais IA, Puopolo M, Yu H (2008) Klotho expression in epithelial ovarian cancer and its association with insulin-like growth factors and disease progression. Cancer Invest 26(2):185–192. https://doi.org/10.1080/07357900701638343

Matsumura Y, Aizawa H, Shiraki-Iida T, Nagai R, Kuro-o M, Nabeshima Y (1998) Identification of the human klotho gene and its two transcripts encoding membrane and secreted klotho protein. Biochem Biophys Res Commun 242(3):626–630. https://doi.org/10.1006/bbrc.1997.8019

Mehi SJ, Maltare A, Abraham CR, King GD (2014) MicroRNA-339 and microRNA-556 regulate Klotho expression in vitro. Age 36(1):141–149. https://doi.org/10.1007/s11357-013-9555-6

Pan JY, Sun CC, Li SJ, Huang J, Li DJ (2015) Role of miR-10b in non-small cell lung cancer (NSCLC) cells by targeting Klotho. Cancer Cell & Microenvironment 2(4):936. https://doi.org/10.14800/ccm.936

Peshes-Yeloz N, Ungar L, Wohl A, Jacoby E, Fisher T, Leitner M et al (2019) Role of Klotho Protein in Tumor Genesis, Cancer Progression, and Prognosis in Patients with High-Grade Glioma. World Neurosurgery 130:324–332. https://doi.org/10.1016/j.wneu.2019.06.082

Rubinek T, Shulman M, Israeli S, Bose S, Avraham A, Zundelevich A et al (2012) Epigenetic silencing of the tumor suppressor klotho

in human breast cancer. Breast Cancer Res Treat 133(2):649–657. https://doi.org/10.1007/s10549-011-1824-4

Shi Y (2004) Caspase activation, inhibition, and reactivation: a mechanistic view. Protein Sci 13(8):1979–1987. https://doi.org/10.1110/ps.04789804

Shu G, Xie B, Ren F, Liu DC, Zhou J, Li Q et al (2013) Restoration of klotho expression induces apoptosis and autophagy in hepatocellular carcinoma cells. Cell Oncol 36(2):121–129. https://doi.org/10.1007/s13402-012-0118-0

Sun H, Gao Y, Lu K, Zhao G, Li X, Li Z et al (2015) Overexpression of Klotho suppresses liver cancer progression and induces cell apoptosis by negatively regulating wnt/β-catenin signaling pathway. World J Surg Oncol 13(1):307. https://doi.org/10.1186/s12957-015-0717-0

Tang X, Wang Y, Fan Z, Ji G, Wang M, Lin J et al (2016) Klotho: a tumor suppressor and modulator of the Wnt/β-catenin pathway in human hepatocellular carcinoma. Lab Invest 96(2):197. https://doi.org/10.1038/labinvest.2015.86

Vaux DL, Silke J (2005) IAPs, RINGs and ubiquitylation. Nat Rev Mol Cell Biol 6(4):287–297. https://doi.org/10.1038/nrm1621

Wang Y, Chen L, Huang G, He D, He J, Xu W et al (2013) Klotho sensitizes human lung cancer cell line to cisplatin via PI3k/Akt pathway. PLoS One 8(2):e57391. https://doi.org/10.1371/journal.pone.0057391

Wolf I, Laitman Y, Rubinek T, Abramovitz L, Novikov I, Beeri R et al (2010) Functional variant of KLOTHO: a breast cancer risk modifier among BRCA1 mutation carriers of Ashkenazi origin. Oncogene 29(1):26. https://doi.org/10.1038/onc.2009.301

Wolf I, Levanon-Cohen S, Bose S, Ligumsky H, Sredni B, Kanety H et al (2008) Klotho: a tumor suppressor and a modulator of the IGF-1 and FGF pathways in human breast cancer. Oncogene 27(56):7094. https://doi.org/10.1038/onc.2008.292

Xie B, Zhou J, Yuan L, Ren F, Liu DC, Li Q et al (2013) Epigenetic silencing of Klotho expression correlates with poor prognosis of human hepatocellular carcinoma. Hum Pathol 44(5):795–801. https://doi.org/10.1016/j.humpath.2012.07.023

Yan Y, Wang Y, Xiong Y, Lin X, Zhou P, Che Z (2017) Reduced Klotho expression contributes to poor survival rates in human patients with ovarian cancer, and overexpression of Klotho inhibits the progression of ovarian cancer partly via the inhibition of systemic inflammation in nude mice. Mol Med Rep 15(4):1777–1785. https://doi.org/10.3892/mmr.2017.6172